Bioconjugate Chemistry

Article

Cite This: Bioconjugate Chem. 2019, 30, 2417−2426

pubs.acs.org/bc

N-Cadherin Mimetic Peptide Nanofiber System Induces Chondrogenic Differentiation of Mesenchymal Stem Cells

Cagla Eren Cimenci,[†] Gozde Uzunalli Kurtulus,[‡] Ozum S. Caliskan,[†] Mustafa O. Guler,[*,§] and Ayse B. Tekinay[*,†,∥,⊥]

[†]Institute of Materials Science and Nanotechnology, National Nanotechnology Research Center (UNAM), Bilkent University, Ankara 06800, Turkey

[‡]Department of Comparative Pathobiology, Purdue University, West Lafayette, Indiana 47907, United States

[§]Pritzker School of Molecular Engineering, University of Chicago, Chicago, Illinois 60637, United States

[∥]Eryigit Biomedical Devices Research and Development Center, Ankara 06380, Turkey

[⊥]Neuroscience Graduate Program, Bilkent University, Ankara 06800, Turkey

Supporting Information

ABSTRACT: Cadherins are vital for cell-to-cell interactions during tissue growth, migration, and differentiation processes. Both biophysical and biochemical inputs are generated upon cell-to-cell adhesions, which determine the fate of the mesenchymal stem cells (MSCs). The effect of cadherin interactions on the MSC differentiation still remains elusive. Here we combined the N-Cadherin mimetic peptide (HAV-PA) with the self-assembling E-PA and the resultant N-cadherin mimetic peptide nanofibers promoted chondrogenic differentiation of MSCs in conjunction with chondrogenic factors as a synthetic extracellular matrix system. Self-assembly of the precursor peptide amphiphile molecules HAV-PA and E-PA enable the organization of HAV peptide residues in close proximity to the cell interaction site, forming a supramolecular N-cadherin-like system. These bioactive peptide nanofibers not only promoted viability and enhanced adhesion of MSCs but also augmented the expression of cartilage specific matrix components compared to the nonbioactive control nanofibers. Overall, the N-cadherin mimetic peptide nanofiber system facilitated MSC commitment into the chondrogenic lineage presenting an alternative bioactive platform for stem-cell-based cartilage regeneration.

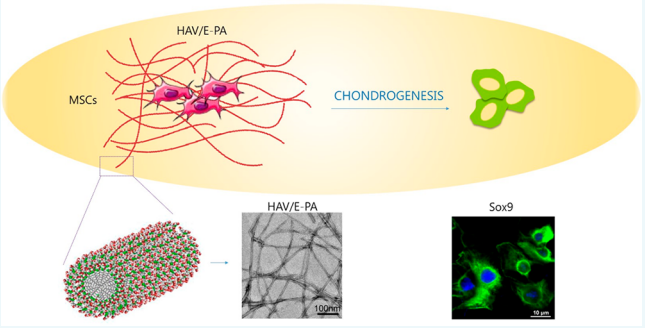

INTRODUCTION

Mesenchymal stem cells (MSCs) are unique for their ability in regeneration of mesenchymal tissues, and they are essential for the development of cellular therapeutics in regenerative medicine applications due to their capacity to self-replicate and form functional tissues.[1,2] These capabilities of MSCs are regulated spatiotemporally by both biochemical and biophysical factors presented by the tissue microenvironment, directing differentiation into specific lineages. Dynamics of the tissue microenvironment can be engineered by utilizing biomaterial scaffold systems, providing bioactive artificial environments for MSC differentiation.[3−5] These biomaterials may either induce or facilitate the chondrogenic differentiation through cell-to-cell and cell-matrix interaction and must present an appropriate combination of biophysical and biochemical characteristics to provide an ideal environment for MSC differentiation into cartilage tissue. Since the extracellular matrix (ECM) has a profound effect on MSC differentiation, many studies have tried to improve the biological functionality of biomaterials by tethering ECM molecules or directly mimicking the ECM structure.[6−9] Thus, discovering novel targets that facilitate the cellular differentiation is highly desirable.

Cadherin molecules are Ca^{2+} dependent type-1 transmembrane glycoproteins that are responsible for maintaining cell and tissue structure and cellular movement through cell adhesion.[10] During chondrogenesis, N-cadherins play an essential role for mesenchymal cell condensation, which is a critical step in tissue morphogenesis.[11,12] N-terminal extracellular domain of the N-cadherin possesses an evolutionarily conserved motif, His-Ala-Val (HAV), which provides a homophilic cell adhesion recognition site that mediates cell-to-cell adhesion.[13] It has been known that inhibition of the HAV motif decreases the N-cadherin dependent cell-to-cell adhesion.[14]

N-Cadherin mediates the aggregation of progenitor cells, promoting cell-to-cell interactions during mesenchymal condensation.[15,16] N-Cadherin deletion also results in decreased cellular condensation and impaired chondrogenesis.[17,18]

Received: July 25, 2019
Published: August 15, 2019

DOI: 10.1021/acs.bioconjchem.9b00514
Bioconjugate Chem. 2019, 30, 2417−2426

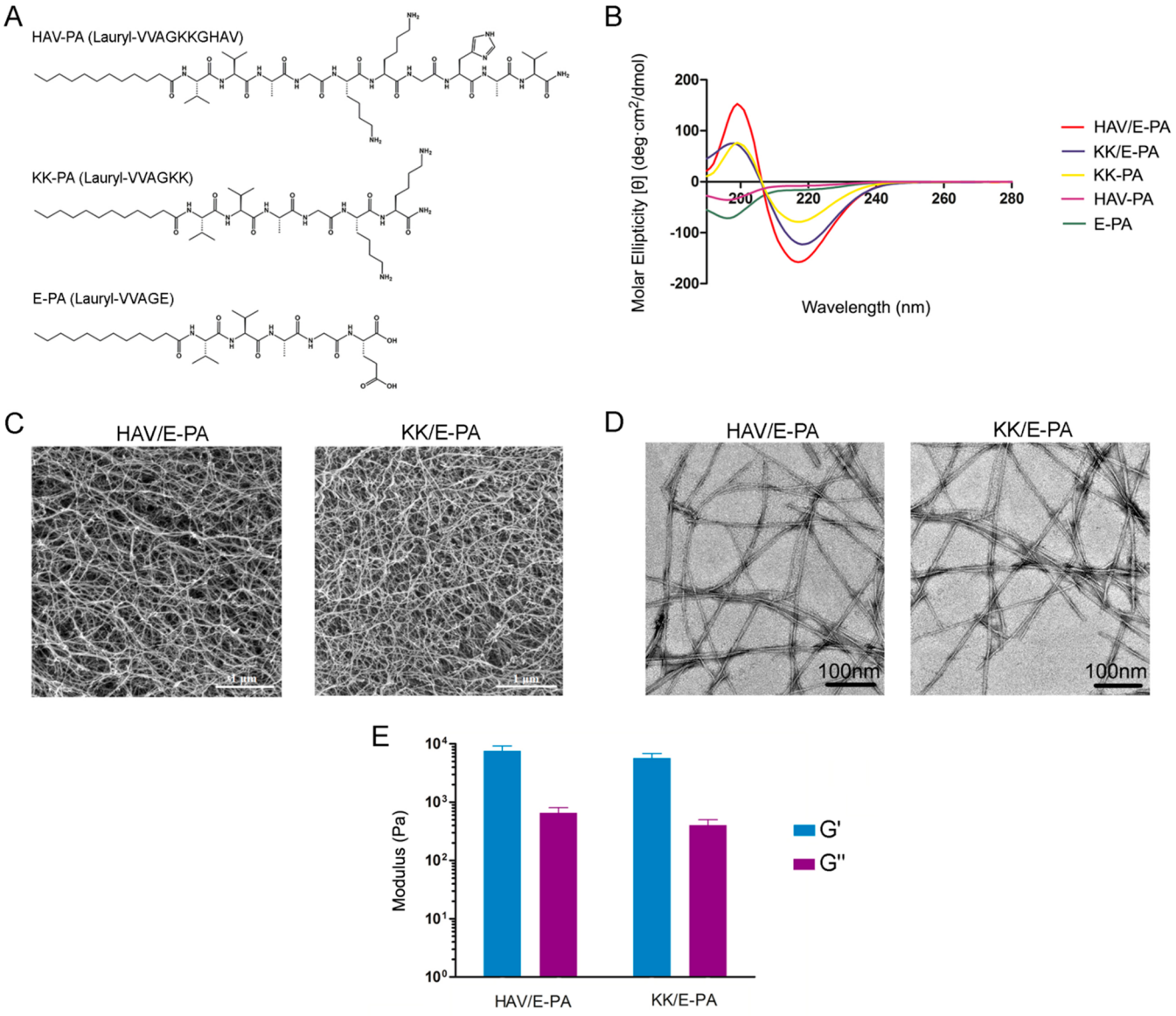

Figure 1. (A) Chemical structures of the peptide amphiphile molecules. (B) Circular dichroism spectroscopy of the PA nanofibers showing β-sheet-like secondary structure. (C) Representative SEM images of HAV/E-PA and KK/E-PA, showing ECM mimetic morphology of the nanofiber networks. (D) Representative TEM image of the HAV/E-PA and KK/E-PA. (E) Rheological characterization of the hydrogels showing storage and loss moduli of HAV/E-PA and KK/E-PA.

During tissue development, morphogenesis, and regeneration, the dynamic remodeling of the ECM components is also required to direct differentiation of uncommitted progenitor cells into a specific lineage. A growing body of evidence suggests that the ECM-cell and cell-to-cell interactions initiate various signal transduction pathways, thereby regulating the lineage of cellular differentiation. This makes cadherin molecules vital for developmental and regenerative processes. While previous relevant studies have shown that HAV sequence bearing peptide derivatives enhance chondrogenesis and osteogenesis of MSCs,[19−21] to the best of our knowledge, our study is the first synthetic ECM-like peptide nanofiber application showing the effect of N-cadherin adhesion on cartilage differentiation.

In this work, we demonstrated an HAV tripeptide sequence presenting the peptide nanofiber system to induce the chondrogenic differentiation of mesenchymal stem cells. The HAV tripeptide sequence containing peptide nanofiber system was designed to mimic the cadherin-like binding interaction for inducing cell-to-cell interactions among MSCs. The designed peptide nanofiber system presented not only cell-binding motifs but also a mechanical architecture, which allows for cellular migration that is necessary for mesenchymal condensation. The N-cadherin mimetic peptide nanofiber system was demonstrated to successfully induce the chondrogenic differentiation of MSCs. Furthermore, when the bioactive epitopes of the peptide nanofiber system were blocked by using a N-cadherin antibody, its chondrogenic effect was also hindered causing reduction of the chondrogenesis related gene expression, which shows the specificity of the matrix and cell interactions. Overall, the chondrogenic differentiation of MSCs was shown to be induced in the presence of cadherin mimetic peptide nanofiber system providing both physical and biological support.

DOI: 10.1021/acs.bioconjchem.9b00514
Bioconjugate Chem. 2019, 30, 2417−2426

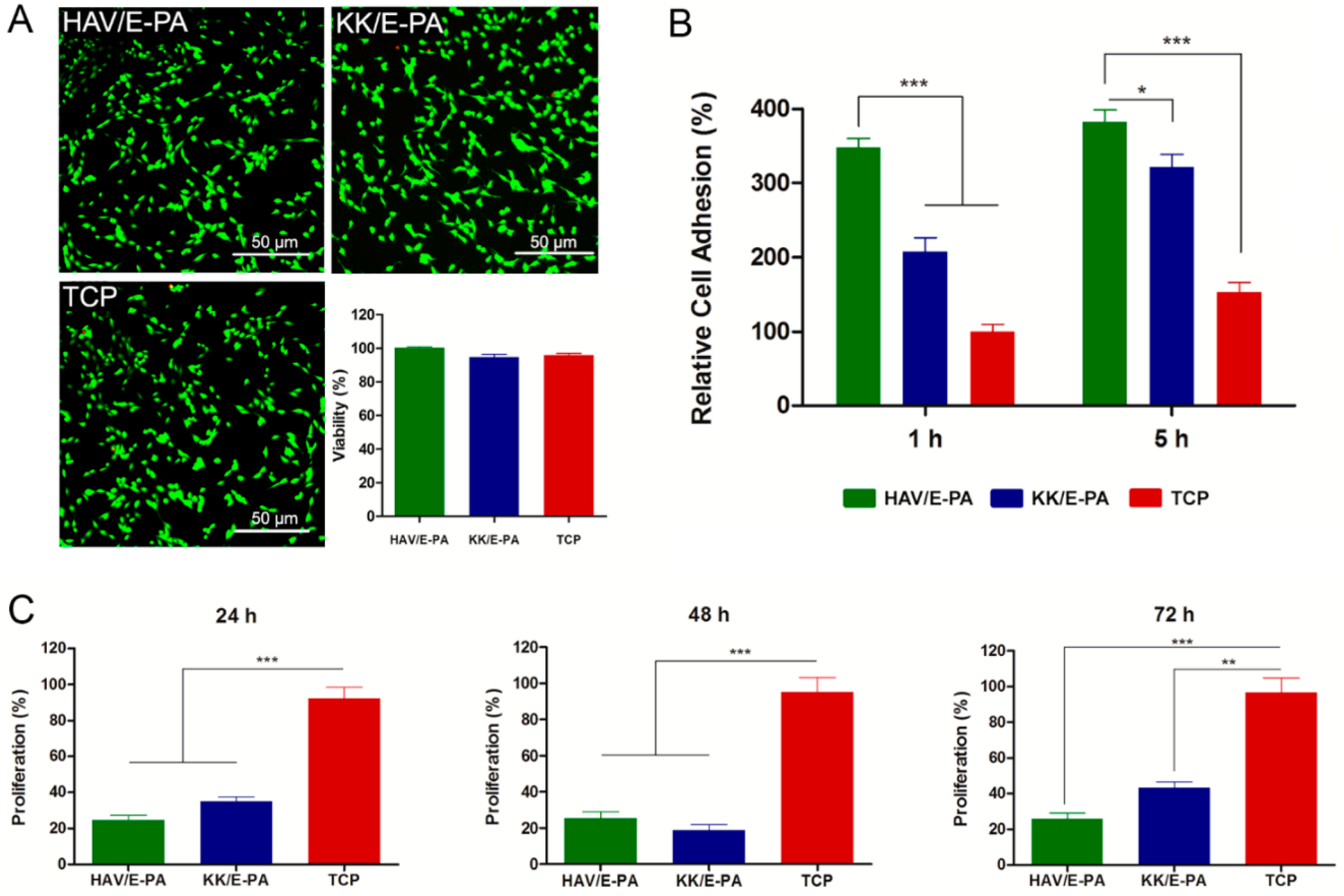

Figure 2. (A) Viability of MSCs on nanofiber networks and TCP at 24 h. Representative live−dead assay images and quantification. (B) Relative cell adhesion of MSCs after 1 and 5 h of incubation in the presence of BSA and cycloheximide. (C) Proliferation rates of MSCs normalized to TCP at 24, 48, and 72 h. Error bars represent mean ± standard error of mean (*p < 0.05, **p < 0.01, and ***p < 0.001).

RESULTS AND DISCUSSION

Synthesis and Characterization of the Peptide Amphiphile Nanofibers. In this study, we exploited the bioactivity of cadherin and the physical support of the ECM by incorporating the evolutionary conservative HAV units into a synthetic peptide nanofiber network. The cadherin mimetic positively charged HAV-PA, negatively charged E-PA, and positively charged KK-PA molecules were synthesized by solid phase peptide synthesis method, purified by preparative HPLC, and characterized by LC−MS prior to their use (Figure S1). The structure of the HAV-PA molecule was designed to mimic cadherin interaction, while E-PA and KK-PA were used as control peptides lacking bioactive epitopes (Figure 1A).

Self-assembly was triggered by mixing negatively charged peptides and positively charged peptides at pH 7.4 to produce neutrally charged peptide networks. This is the main advantage of our supramolecular peptide hydrogel system, allowing the self-assembly without linker usage or any external force. Hydrophobic site of the PA molecules, composed of a long alkyl chain, induces hydrophobic collapse and remains in the interior part of the nanofiber structure. Hydrophilic peptide segment enables solubility in water and presents a bioactive peptide sequence on the surface of the self-assembled nanostructures. Following the self-assembly, secondary structures of peptide amphiphiles and their mixtures were characterized by circular dichroism (CD) analysis. Both cadherin-mimetic peptide nanofiber system and the control nanofibers showed predominantly β-sheet structures with a minimum at around 220 nm and maximum around 200 nm, showing the structural properties of the gels were comparable (Figure 1B). The scanning electron microscopy (SEM) imaging of the self-assembled PA nanofibers indicated that both HAV/E-PA and KK/E-PA show meshlike morphology at the microscale level (Figure 1C). The structures of individual nanofibers were observed under transmission electron microscopy, which revealed the presence of high-aspect-ratio nanofibers with diameters of around 10 nm and lengths reaching several micrometers (Figure 1D). Mechanical properties of the extracellular environment are crucial for determining cell fate, and thus we studied the gels by using oscillatory rheology. The mechanical characterization of nanofiber systems showed that the storage moduli were greater than loss moduli, indicating self-supporting gel formation (Figure 1E). The peptide gels exhibited storage moduli of ∼9 kPa and loss moduli of ∼0.9 kPa. Overall, our findings suggest that both HAV/E-PA and KK/E-PA biomaterial scaffold systems bear suitable mechanical properties to be able to support chondrogenic differentiation as our material is neither considered as a soft material (≤1 kPa) which is ideal for brain cells nor a stiff material (≥20 kPa) which is considered an ideal surface for osteocyte differentiation.[22−24]

Cellular Behavior Analyses. The biocompatibility of the nanofiber networks was investigated by examining the viability

DOI: 10.1021/acs.bioconjchem.9b00514
Bioconjugate Chem. 2019, 30, 2417−2426

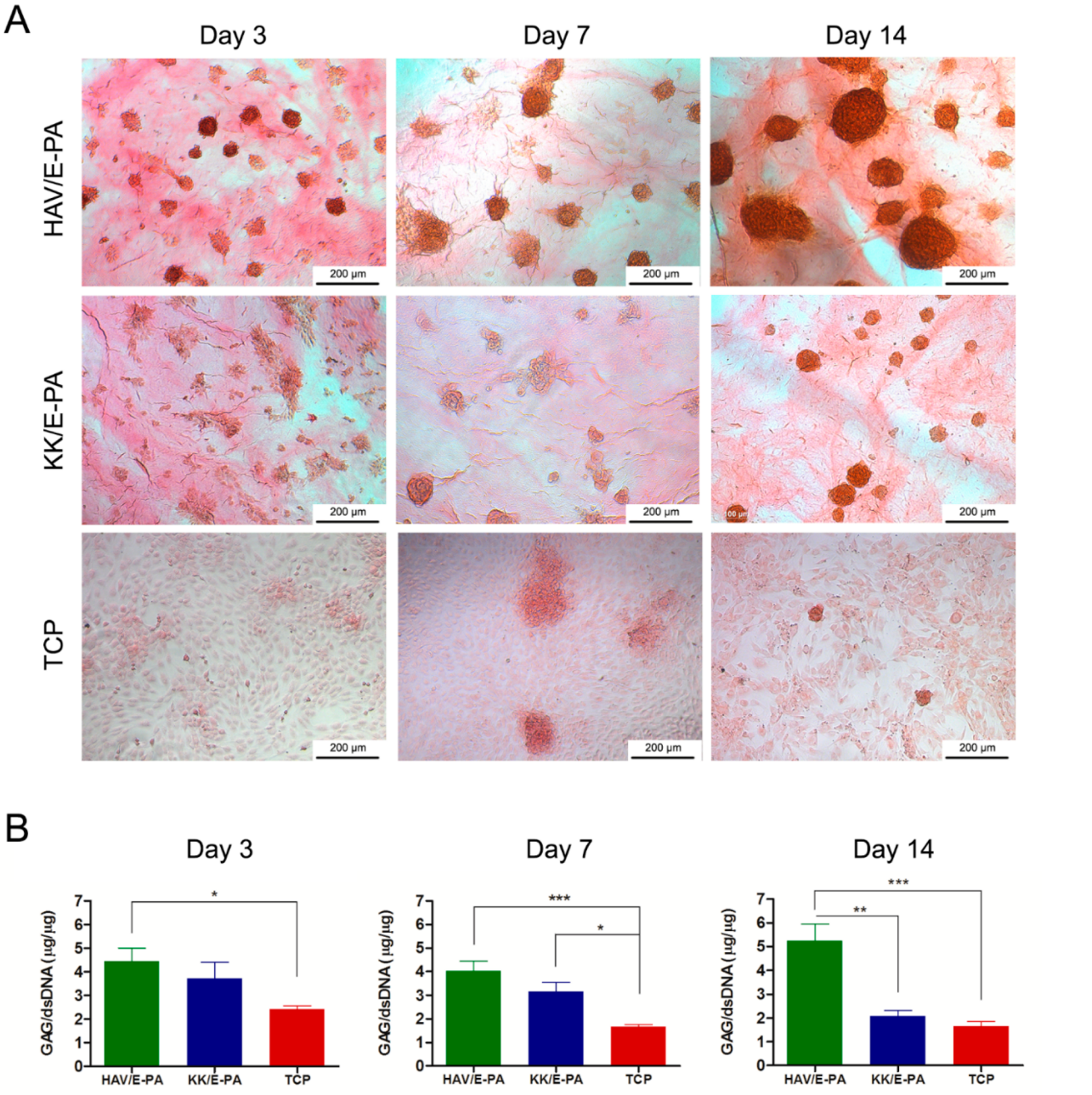

Figure 3. Glycosaminoglycan deposition of MSCs on nanofiber networks or uncoated TCP on days 3, 7, and 14. (A) Safranin-O staining shows the deposition of sulfated GAG content. (B) DMMB assay shows the quantification of the sulfated GAG deposition. GAG content was normalized to dsDNA content and was expressed as $\mu g/\mu g$. Error bars represent standard error of mean (*$p < 0.05$, **$p < 0.01$, and ***$p < 0.001$).

of the MSCs cultured on peptide nanofibers for 24 h (Figure 2A). Calcein AM and ethidium homodimer staining were performed to determine the number of viable and dead cells, while bare tissue culture plates were used as the control. Cellular viability rates were comparable between the bare surface and the nanofiber-coated surfaces, suggesting that the nanofiber networks are biocompatible.

We also investigated the adhesive behavior of the cells to the nanofibrous networks in the presence of a translation inhibitor, cycloheximide, which minimizes the interference of the endogenous proteins during adhesion process (Figure 2B). After 1 and 5 h of culture, cells on the cadherin-mimetic surfaces were found to adhere significantly better than the uncoated TCP and the control nanofiber group. Incorporation of the bioactive signals into the peptide nanofiber system significantly supported the adhesion profile, indicating better cellular adaptation on the cadherin-mimetic surface. The cadherin-mimetic nanofibrous system also mimics the fibrous ECM, which is responsible for regulating the cell adhesion and protein adsorption processes.

The effects of the cadherin-mimetic PA nanofibers on the MSC proliferation was assayed by using a BrdU-based proliferation assay (Figure 2C). The proliferation rates of MSCs on both HAV/E-PA and KK/E-PA nanofibers were significantly lower compared to TCP at 24 and 48 h of culture. However, after 72 h, cellular proliferation rate on HAV/E-PA nanofibers was significantly lower than both TCP and the nonbioactive group. Although all experimental groups showed

DOI: 10.1021/acs.bioconjchem.9b00514
Bioconjugate Chem. 2019, 30, 2417−2426

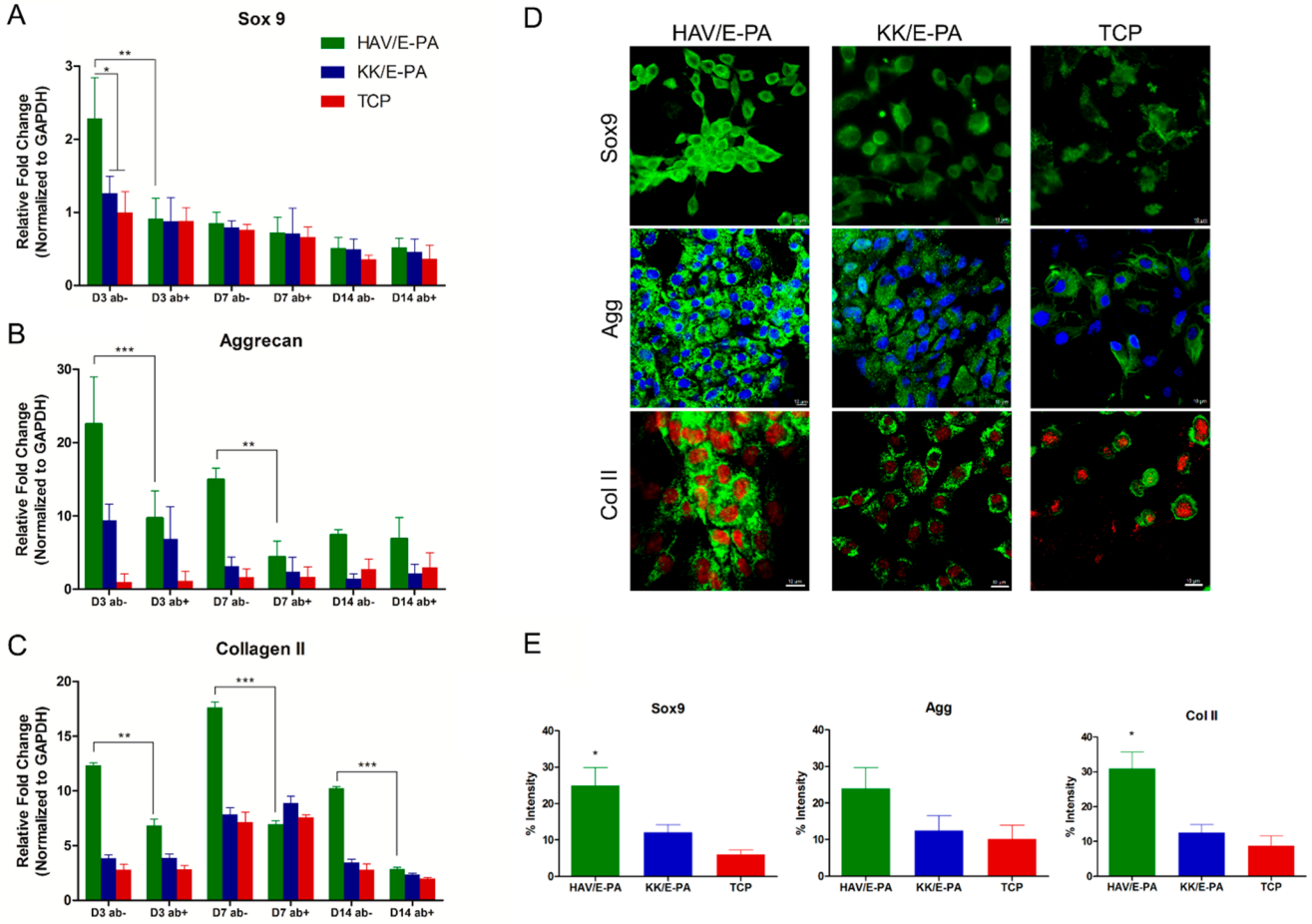

Figure 4. Cartilage specific gene and protein expression profile of MSCs. HAV/E-PA enhances early rMSC chondrogenesis. (A) Sox9, (B) Aggrecan, and (C) Collagen II expression of MSCs on both nanofiber networks and TCP after 3, 7, and 14 days of in vitro culture in chondrogenic media either untreated (ab-) or with treatment of the N-cadherin antibody (ab+). (D) Sox9, Aggrecan, and Collagen II expression of MSCs on HAV/E-PA, KK/E-PA, and TCP surfaces after 7 days. (E) Quantification of ICC data as % of intensity. Statistical analysis was performed with one-way ANOVA and Bonferroni's multiple comparisons test. Error bars represent standard error of mean. Scale bars are 10 μm for each ICC image.

similar effects on MSCs in terms of viability, HAV/E-PA coated surface impeded cell proliferation significantly since MSCs are required to exit the cell cycle prior to differentiation.[25] Overall, the combination of these factors allows the HAV/E-PA system to provide a biocompatible and bioinductive environment for the culturing of MSCs.

N-Cadherin Mimetic Peptide Nanofiber Network Enhances MSC Aggregation and Deposition of Cartilage ECM Components. We also analyzed the chondrogenic differentiation potential of MSCs on the nanofiber networks. Chondrocyte lineage-committed MSCs start to deposit sulfated glycosaminoglycans and increase cell−cell interactions, as evidenced by aggregate formation.[26−28] The deposition of sulfated glycosaminoglycans (GAG) was examined by Safranin-O staining and quantified with dimethylmethylene blue (DMMB) assay on days 3, 7, and 14. Prominent staining on cellular aggregates indicated the accumulation of GAGs in HAV/E-PA group, whereas cells on KK/E-PA and TCP were stained less specifically (Figure 3A). Aggregations began to form on day 3 for the HAV/E-PA group, whereas they first were observed after 7 days in the KK/E-PA and TCP groups. Especially on day 14, cellular aggregates were larger and more intense in color after Safranin-O staining in the cadherin-mimetic peptide coating group, indicating abundant GAG accumulation. Some aggregate formation was observed in KK/E-PA as well; however, they were less in number and smaller in size compared to HAV/E-PA. Since some previous studies suggested that aggregate formation may not be necessary to induce chondrogenesis itself,[29,30] we conducted further assays and found that the DMMB results also correlate well with the results we observed in Safranin-O staining, indicating that the GAG/dsDNA content was higher on the HAV/E-PA group compared to the other groups on days 3 and 7, while it was also higher on the KK/E-PA group compared to TCP samples (Figure 3B). Strikingly, on day 14, the accumulation of glycosaminoglycan per DNA was two times higher in cells on the HAV/E-PA group compared to cells cultured on KK/E-PA and TCP, suggesting that the cadherin-mimetic peptide nanofiber network promoted GAG deposition. It has previously been shown that after cadherin-mediated cell−cell adhesions begin to form, they become progressively stronger, leading to the formation of larger aggregates.[31] Consistently, our evidence indicates that the cadherin-mimetic peptide nanofiber network enhances MSC aggregation and the deposition of cartilaginous matrix components in vitro.

Gene Expression Analyses Confirm Chondrogenic Lineage Commitment. Morphological observations clearly showed that the MSCs formed aggregates within 3 days following their seeding on N-cadherin mimetic peptide nanofibers, suggesting a rapid commitment to the chondro-

DOI: 10.1021/acs.bioconjchem.9b00514
Bioconjugate Chem. 2019, 30, 2417−2426

genic lineage. Morphological changes and deposition of cartilage ECM components were confirmed by gene expression analyses on days 3, 7, and 14. Gene expression analysis revealed that the commitment of the MSCs to the chondrogenic lineage on the cadherin mimetic HAV/E-PA surface was enhanced compared to cells on KK/E-PA and TCP. The expression levels of the chondrogenic markers Sox9, Aggrecan, and Col II on days 3, 7, and 14 in the HAV/E-PA group were significantly higher than the control and TCP groups (Figure 4, panels A−C). No significance was observed between the control and TCP groups. Sox9 is a transcription factor which activates an enhancer in the gene of type II collagen,[32] and the expression of Sox9 in the HAV/E-PA group was increased by 1.75-fold on day 3, leading the increase of the Col II expression by 2.42-fold and 2.85-fold on days 7 and 14, respectively, leading an increase in the Col II expression on the following days. Collagen type II preferentially promotes ECM deposition and the formation of fibrillary structures during chondrogenesis.[33,34] Aggrecan is another critical component for cartilage structure, which is a proteoglycan and is crucial in chondroskeletal morphogenesis.[35] Proliferating chondrocytes express the chondrocyte specific ECM protein Aggrecan,[36] and Sox9 enhances the induction of the gene that encodes Aggrecan as well.[37,38] Accordingly, our results showed that the Aggrecan expression was significantly increased by 2.3-fold and 4.7-fold on days 3 and 7, respectively, indicating that the chondrogenic differentiation rate was increased during that time.

Furthermore, we showed that the N-cadherin antibody treatment eliminated the chondrogenic effect of the HAV peptides, causing a reduction of the expression of chondrogenic genes Sox9, Agg, and Col II to similar levels with the control group. The qRT-PCR results were consistent with the previous studies, which shows that the N-cadherin antibody treatment abrogated the chondrogenic ability of N-cadherin peptides and reduced the expression of chondrogenic genes to levels similar to those of the control group.[20] We also investigated cartilage specific protein expressions by immunolocalization with fluorescence-conjugated antibodies on day 7. Confocal microscopy of the immunostained MSC aggregates showed the localization of Sox9, Aggrecan, and Collagen II proteins on rMSCs on HAV/E-PA, KK/E-PA, and TCP on day 7, indicating that the deposition of chondrogenic markers are more prominent in HAV/E-PA group compared to KK/E-PA and TCP (Figure 4D). We also quantified % of intensity in fluorescence signals on day 7. N-Cadherin mimicking the HAV/E-PA group showed significantly higher intensities of Sox9 and Col II, indicating an upregulation of cartilage specific markers. On the other hand, while Agg exhibited a higher intensity profile in HAV/E-PA group, we did not observe any significant differences between groups on day 7.

As Sox9 is a transcription factor, which translocates to the nuclei during chondrogenesis,[38,39] we also quantified nuclear versus cytoplasmic expression intensities of Sox9 (Figure S2). The results of this analysis showed that the ratio of % intensity (nuclei/cytoplasm) was significantly greater in the HAV/E-PA group compared to KK/E-PA and TCP groups, which shows higher nuclear compartmentalization of Sox9. This translocation also indicates chondrocyte differentiation from mesenchymal progenitors.[40]

Overall, these findings suggested that the chondrogenic differentiation was enhanced by the N-cadherin mimetic HAV/E-PA, stimulating the expression of cartilage-specific markers, including Sox9, Aggrecan, and type II collagen, by creating a biomimetic environment for chondrogenesis. In addition to the biochemical cues provided by the cadherin mimetic sequence, the nanofiber structure of the HAV/E-PA matrix itself may assist in differentiation and proliferation of MSCs into chondrocytes.

■ CONCLUSION

In summary, we demonstrated that the cadherin mimetic HAV peptide nanofibers are able to support the differentiation of the mesenchymal stem cells into chondrocytes by facilitating their commitment to the chondrogenic lineage. The HAV peptide sequence conjugated HA hydrogels promoted chondrogenesis of the encapsulated MSCs.[20] In this work, we demonstrated the effect of N-cadherin mimetic ECM-like peptide nanofiber systems on regulating chondrogenic differentiation of MSCs for the first time. We have shown that the combination of biological (N-Cadherin mimetic HAV motif) and physical (amphiphilic peptide nanofiber system) cues facilitated the mesenchymal condensation and chondrogenesis. Our results showed that stem cell differentiation can be guided by using cadherin mimetic bioactive ECM mimetic materials for further stem cell based cartilage regeneration studies.

■ EXPERIMENTAL PROCEDURES

Materials. [4-[-(2′,4′-Dimethoxyphenyl) Fmoc-aminomethyl]phenoxy] acetamidonorleucyl-MBHA resin (Rink amide MBHA resin), Fmoc-Glu(OtBu)-Wang resin, 2-(1HBenzotriazol-1-yl)-1,1,3,3-tetramethyluronium hexafluorophosphate (HBTU), 9-fluorenylmethoxycarbonyl (Fmoc), and tert-butoxycarbonyl (Boc) protected amino acids were purchased from NovaBiochem, ABCR, and Sigma-Aldrich. Fmoc-Ser[-Glc(OAc)4]-OH was purchased from AAPPTec. N,N-Diisopropylethylamine (DIEA) and lauric acid were purchased from Merck. Piperidine, acetic anhydride, dichloromethane (DCM), dimethylformamide (DMF), trifluoroacetic acid (TFA), and triisoproplysilane (TIS) were obtained from Sigma-Aldrich. All other chemicals and materials were purchased from Invitrogen, Fisher, Merck, Alfa Aesar, and SigmaAldrich. Deionized water (ddH_2O) used in the experiments had a resistance of 18.2 MΩ cm (Millipore Milli-Q). All chemicals and materials were used as provided. For cell culture experiments, Dulbecco's Modified Eagle Medium (DMEM), Penicillin/Streptomycin (PS) antibiotic mix, and Fetal Bovine Serum (FBS) were purchased from Gibco, Life Technologies. The LIVE/DEAD Viability/Cytotoxicity Kit was purchased from Invitrogen. Safranin-O was obtained from Sigma-Aldrich. All other chemicals and materials used in this study were purchased from Invitrogen, Merck, Thermo Scientific, or Sigma. All the chemicals were used as provided.

Methods. *Peptide Amphiphile Synthesis, Purification and Characterization.* Peptide amphiphile (PA) molecules were synthesized by a standard solid phase peptide synthesis (SPPS) method. HAV-PA [Lauryl-VVAGKKGHAV-Am] and KK-PA [Lauryl-VVAGKK-Am] were constructed on MHBA Rink Amide resin, and E-PA [Lauryl-VVAGE] was constructed on Wang resin preloaded with Fmoc-Glu (OtBu). The resins were swelled in DCM for 30 min and following resin swelling, DCM solvent was exchanged to DMF, in which all remaining reactions were carried out. All amino acid couplings were performed with 2 equiv of Fmoc protected amino acid, 1.95 equiv of HBTU, and 3 equiv of N,N-diisopropylethylamine

DOI: 10.1021/acs.bioconjchem.9b00514
Bioconjugate Chem. 2019, 30, 2417−2426

(DIEA) in DMF. The coupling duration was at least 3 h but varied depending on the type of the amino acid that was coupled. Equivalences were based on the resin that was used for construction.

Fmoc deprotections were performed by using 20% piperidine/dimethylformamide (DMF) solution for 20 min. After each coupling reaction, the resin was treated with 10% acetic anhydride in DMF for 30 min to block any remaining free amino groups. Before each succeeding event, washing was performed by DMF, DCM, and DMF, respectively, three times each. Cleavage of the peptides from the resin was carried out with a mixture of TFA:TIS:water in the ratio of 95:2.5:2.5 for 2 h. Excess TFA was removed by rotary evaporation. The remaining viscous peptide solution was treated with ice-cold diethyl ether overnight at −20 °C. Ether decantation was performed after centrifugation at 4 °C, 8000 rpm, for 15 min. After complete evaporation of diethyl ether via air drying, the resulting pellet was dissolved in ddH_2O, sonicated for 30 min, freeze-dried at −80 °C, and lyophilized. The PAs were stored at −20 °C.

The synthesized peptide was characterized by liquid chromatography mass spectrometry (LC−MS) on an Agilent 6530 Q-TOF mass spectrometer equipped with ESI source and reverse phase analytical high performance liquid chromatography. Basic conditions and acidic conditions were used to identify the negatively charged and positively charged PA molecules, respectively. For basic conditions, a Zorbax Extend-C18 (4.6 × 50 mm) column and water/acetonitrile gradient with 0.1% volume of NH_4OH were used. For acidic conditions, a Zorbax 300 SB-C8 (4.6 × 100 mm) column and water/acetonitrile gradient with 0.1% volume of formic acid were used. An Agilent 1200 preparative reverse-phase HPLC system was used for the purification of the PA molecules. As a stationary phase, a Luna 5u C8 (2) (21.20 × 100 mm) column for acidic conditions and a Gemini 5u C18 (21.20 × 100 mm) column for basic conditions was used to purify the negatively charged and the positively charged PA molecules, respectively. For the mobile phase, a water/acetonitrile gradient with a 0.1% volume of NH_4OH for basic conditions and a water/acetonitrile gradient with 0.1% volume of TFA for acidic conditions were used.

Formation of Peptide Amphiphile Nanostructures, Spectroscopic, and Morphological Characterizations. The PA solutions were prepared by mixing two oppositely charged PA solutions at 1 mM concentration which resulted in the peptide hydrogel formation. In order to form neutrally charged peptide nanofibers, positively charged bioactive HAV-PA and negatively charged E-PA (at pH 7.4) were mixed to form bioactive nanofibers at a 1:1 molar ratio. To form control nonbioactive nanofibers, positively charged nonbioactive KK-PA and negatively charged E-PA (at pH 7.4) were mixed at a 1:1 molar ratio. PA solutions were sonicated for 15 min and sterilized under UV for 15 min.

The secondary structures of the PA molecules were characterized by a J-815 Jasco circular dichroism spectrophotometer in the far ultraviolet region using quartz cuvettes with a 1 mm path length. The PA solutions were dissolved in deionized water at a concentration of 0.01% w/v, and the pH was adjusted to 7.4. The CD spectra of HAV-PA, KK-PA, E-PA, HAV/E-PA, and KK/E-PA (1:1 volume ratio) were obtained from scanning at 190 to 300 nm using a digital integration time of 1 s, a bandwidth of 1 nm, and with standard sensitivity. The results were obtained as molar ellipticity and converted into the unit of deg cm^2 $dmol^{-1}$ using the equation of $[\theta] = (100 \times \Omega)/(C \times 0.l)$ where Ω is the obtained value, C is the concentration in molar, and 0.l is the cell path length in centimeters.

For scanning electron microscopy (SEM) imaging, the peptide hydrogels were prepared on cleaned silica wafers. Obtained gels were incubated for 20 min at room temperature to allow gelation and then were dehydrated. Dehydration was performed in 20, 40, 60, 80, and 100% ethanol solutions sequentially. The dehydrated gels were dried with a Tousimis Autosamdri-815B critical-point-drier to preserve the network structure. The samples were then coated with 5 nm layer of Au/Pd and visualized under high vacuum with a FEI Quanta 200 FEG SEM equipped with an ETD detector.

Transmission electron microscopy (TEM) samples were prepared on a 200-mesh cupper TEM grid. Nanostructures were formed as explained above, and these solutions were 10 times diluted. Thirty microliters from the solutions were dropped on a parafilm, and the grid was placed onto a droplet. After a 5 min incubation, the grid was taken, excess PA solution was removed, and the grid was stained with 2 wt % uranyl-acetate for 3 min. Immediately after 3 min, the uranyl-acetate was removed, the grid was rinsed with ddH_2O and left to air dry. TEM images were acquired with a FEI Tecnai G2 F30 TEM at 300 kV.

rMSC Culture and the Preparation of Nanofibrous Networks for in Vitro Culture. Rat mesenchymal stem cells (rMSCs) (Invitrogen) were expanded in a maintenance medium consisting of DMEM supplemented with 10% (v/v) FBS (Invitrogen), 1% (v/v) GlutaMAX (Invitrogen), and 1% PS (Invitrogen). Chondrogenic differentiation was induced with a StemPro Chondrogenesis Differentiation Kit (Invitrogen). All experiments were conducted with cells between passages 7−9. Cells were maintained at a standard cell culture environment (5% CO_2, 37 °C) in humidified incubators. Cells were passaged at 80% confluency by Trypsin-EDTA (0.025%) (Invitrogen) and reseeded at 3000 cells/cm^2. The culture medium was replaced every 3−4 days. rMSCs were seeded on PA-coated surfaces or uncoated culture plates. The PA coating of the plates was performed by mixing oppositely charged 1 mM PA solutions at a ratio of 150 μL/cm^2. Coated plates were dried under a laminar flow hood for 16 h and sterilized under UV irradiation for 30 min before cell seeding.

Cell Viability, Proliferation, and Adhesion. Cellular viability was assessed using a Live−Dead assay kit (Invitrogen). Cells were seeded on 96-well plates and incubated for 24 h. Then, they were stained with a 2 μM Calcein AM and 4 μM ethidium homodimer cocktail in phosphate-buffered saline (PBS) for 30 min at room temperature in the dark. Stained cells were observed under a fluorescence microscope, and the cell numbers were counted using ImageJ software (NIH, USA). Fifteen random images were taken for each experimental and control group, and the average number of cells on each well were calculated.

The proliferation of the cells was assessed using BrdU assay (Roche). Cells were seeded onto PA-coated wells and uncoated tissue culture plates (TCP) at a density of 3×10^3 cells/well. Cells were incubated in standard cell culture medium supplemented with 100 μM BrdU labeling solution for 24, 48, and 72 h. At the end of the incubation, BrdU incorporation assay was performed according to the manufacturer's instructions. Proliferation rates of the cells

DOI: 10.1021/acs.bioconjchem.9b00514
Bioconjugate Chem. 2019, 30, 2417−2426

were quantified by measuring the absorbance (370 nm, with 492 nm reference wavelength) with a microplate reader.

The adhesion of the rMSCs was assessed at 1 and 5 h after seeding cells on each peptide network and glass surface. Prior to the experiment, cells were pretreated with 50 μg/mL cycloheximide in a serum-free DMEM medium supplemented with 4 mg/mL BSA for 1 h at 37 °C and 5% CO_2 to eliminate the effect of the endogenous proteins in initial cell attachment onto surfaces. Then, they were removed from the tissue culture plate by trypsinization and seeded onto the coated 96-well plates. After 2 h incubation in serum-free medium at standard culture conditions, Calcein AM (Invitrogen) staining (2 μM) was performed for 40 min according to the manufacturer's instructions. Images were taken from 5 different random locations per well, and the experiment was carried out with n = 3. Cell adhesion was quantified directly by counting the number of cells using ImageJ software. The results were then normalized to TCP counts.

Detection of Glycosaminoglycan Deposition and Quantitative Analysis. Glycosaminoglycan (GAG) deposition was evaluated through Safranin-O staining at the end of the days 3, 7, and 14. Culture medium was discarded, and cells were washed with PBS and were fixed with 4% paraformaldehyde for 15 min at room temperature. After washing with PBS, samples were blocked with 1% (w/v) BSA/PBS for 30 min at room temperature and then stained with 0.1% (w/v) Safranin-O in 1% (v/v) acetic acid for 5 min at room temperature. Cells were washed with 0.1% (v/v) acetic acid in PBS extensively to remove the unbound dye, and the sulfated GAG deposition was observed under a light microscope.

The quantification of the sulfated glycosaminoglycans (sGAG) was performed using the dimethyl methylene blue (DMMB) assay on days 3, 7, and 14. First, the culture medium was removed and cells were washed with 1× PBS. The samples were treated with papain digestion buffer containing 100 mM sodium phosphate buffer, 10 mM Na_2EDTA, 10 mM L-cysteine, and 0.125 mg/mL papain for 16 h at 65 °C. In order to measure the amount of GAG production per DNA content, total dsDNA per well was also measured (n = 5). DNA amount of each sample was determined using Qubit dsDNA quantification kit (Invitrogen) according to the manufacturer's instructions. The sGAG amount was calculated from a standard curve that was generated using diluted chondroitin sulfate standards (from 0 to 35 μg mL^{-1}). Then, DMMB dye was prepared by using 16 mg L^{-1} 1,9-dimethylmethylene blue, 40 mM glycine, 40 mM NaCl, and 9.5 mM HCl (pH 3.0), and 100 μL of the dye solution was added onto 40 μL of papain-digested solutions and standard samples. The sGAG concentration was determined by measuring the change in absorbance of the DMMB solution at 595 nm. Finally, GAG/dsDNA content was calculated for each experimental group after days 3, 7, and 14.

Gene Expression Analysis. For analyzing chondrogenic differentiation, gene expression profiles of rMSCs were assessed by quantitative real time PCR (qRT-PCR). To observe the direct effect of cadherin peptides on chondrogenesis, mesenchymal stem cells were divided into two groups. One of the groups was treated with an N-cadherin antibody, while the other group remained untreated. RNA from each sample was isolated with TRIzol reagent (Invitrogen) according to the manufacturer's instructions. Purity and yield of isolated RNA were determined with Nanodrop 2000 spectrometer (Thermo Scientific). Both cDNA synthesis and qRT-PCR were performed with a one-step qRT-PCR kit (SuperScript III Platinum SYBR Green) according to the manufacturer's instructions. Primer sets that were used in this study are shown in Table S1. The relative gene expression was calculated using the ΔΔCT method, where the fold difference was calculated using the expression 2ΔΔCt, and normalized to GAPDH.

Immunostaining and Imaging. To investigate the expression of chondrogenic markers at day 7, rMSCs were fixed in 4% paraformaldehyde/PBS for 10 min and then cells were permeabilized with 0.1% Triton X-100 for 15 min. For blocking, samples were incubated with 10% (w/v) bovine serum albumin/PBS for 30 min and treated with Collagen II primary antibody (Abcam) at 1:200 dilution or Aggrecan antibody at 1:200 dilution (Abcam) or Sox9 primary antibody (Abcam) at 1:300 dilution overnight at 4 °C. Cells were then washed with 1× PBS and incubated for 1 h at room temperature with Goat Anti-Rabbit IgG H&L (Alexa Fluor 488 − Abcam 150077). All samples were counterstained with 1 μM TO-PRO-3 (Invitrogen) in PBS for 20 min at room temperature and mounted with Prolong Gold Antifade Reagent (Invitrogen) with a coverslip. Samples were imaged using a Zeiss LSM510 confocal system.

Statistical Analysis. Results were expressed as mean ± standard deviation. Either one-way analysis of variance (ANOVA) or two-way ANOVA with Tukey's/Bonferroni's Multiple Comparison Test (GraphPad Prism v5) was used to compare the values between the study groups. Paired and nonpaired t test were also applied to describe the association between the study groups. A value of $p \leq 0.05$ was considered to be statistically significant.

■ ASSOCIATED CONTENT

Supporting Information

The Supporting Information is available free of charge on the ACS Publications website at DOI: 10.1021/acs.bioconjchem.9b00514.

Reverse-phase HPLC chromatogram of the HAV-PA molecule, KK-PA, and E-PA; primer sequences used for qRT-PCR expression analysis; and quantification as % intensity of Sox9 chondrogenic marker in day 7 and ratio of % intensity showing nuclei/cytoplasm (PDF)

■ AUTHOR INFORMATION

Corresponding Authors

*E-mail: mguler@uchicago.edu.
*E-mail: atekinay@bilkent.edu.tr.

ORCID

Mustafa O. Guler: 0000-0003-1168-202X
Ayse B. Tekinay: 0000-0002-4453-814X

Notes

The authors declare no competing financial interest.

■ ACKNOWLEDGMENTS

We would like to thank Mr. M. Guler for help in TEM imaging and Ms. Z. Erdogan for LC−MS analysis. C.E.C. was supported by TUBITAK BIDEB 2210-C graduate fellowship. A.B.T. acknowledges support from the Science Academy Outstanding Young Scientist Award (BAGEP).

DOI: 10.1021/acs.bioconjchem.9b00514
Bioconjugate Chem. 2019, 30, 2417−2426

REFERENCES

(1) Law, S., and Chaudhuri, S. (2013) Mesenchymal stem cell and regenerative medicine: regeneration versus immunomodulatory challenges. *Am. J. Stem Cells 2*, 22−38.

(2) Schäfer, R., Spohn, G., and Baer, P. (2016) Mesenchymal Stem/Stromal Cells in Regenerative Medicine: Can Preconditioning Strategies Improve Therapeutic Efficacy? *Transfus Med. Hemother 43*, 256−267.

(3) Lutolf, M. P., Gilbert, P. M., and Blau, H. M. (2009) Designing materials to direct stem-cell fate. *Nature 462*, 433−441.

(4) Huang, A. H., Farrell, M. J., and Mauck, R. L. (2010) Mechanics and mechanobiology of mesenchymal stem cell-based engineered cartilage. *J. Biomech 43*, 128−136.

(5) Diao, H., Wang, J., Shen, C., Xia, S., Guo, T., Dong, L., Zhang, C., Chen, J., Zhao, J., and Zhang, J. (2009) Improved cartilage regeneration utilizing mesenchymal stem cells in TGF-beta1 gene-activated scaffolds. *Tissue Eng., Part A 15*, 2687−2698.

(6) Ustun Yaylaci, S., Sardan Ekiz, M., Arslan, E., Can, N., Kilic, E., Ozkan, H., Orujalipoor, I., Ide, S., Tekinay, A. B., and Guler, M. O. (2016) Supramolecular GAG-like Self-Assembled Glycopeptide Nanofibers Induce Chondrogenesis and Cartilage Regeneration. *Biomacromolecules 17*, 679−689.

(7) Lee, H. J., Yu, C., Chansakul, T., Hwang, N. S., Varghese, S., Yu, S. M., and Elisseeff, J. H. (2008) Enhanced chondrogenesis of mesenchymal stem cells in collagen mimetic peptide-mediated microenvironment. *Tissue Eng., Part A 14*, 1843−1851.

(8) Arslan, E., Guler, M. O., and Tekinay, A. B. (2016) Glycosaminoglycan-Mimetic Signals Direct the Osteo/Chondrogenic Differentiation of Mesenchymal Stem Cells in a Three-Dimensional Peptide Nanofiber Extracellular Matrix Mimetic Environment. *Biomacromolecules 17*, 1280−1291.

(9) Arslan, E., Garip, I. C., Gulseren, G., Tekinay, A. B., and Guler, M. O. (2014) Bioactive supramolecular peptide nanofibers for regenerative medicine. *Adv. Healthcare Mater. 3*, 1357−1376.

(10) Tepass, U., Truong, K., Godt, D., Ikura, M., and Peifer, M. (2000) Cadherins in embryonic and neural morphogenesis. *Nat. Rev. Mol. Cell Biol. 1*, 91−100.

(11) Delise, A. M., and Tuan, R. S. (2002) Analysis of N-cadherin function in limb mesenchymal chondrogenesis in vitro. *Dev. Dyn. 225*, 195−204.

(12) Richardson, S. H., Starborg, T., Lu, Y., Humphries, S. M., Meadows, R. S., and Kadler, K. E. (2007) Tendon development requires regulation of cell condensation and cell shape via cadherin-11-mediated cell-cell junctions. *Mol. Cell. Biol. 27*, 6218−6228.

(13) Blaschuk, O. W., Sullivan, R., David, S., and Pouliot, Y. (1990) Identification of a cadherin cell adhesion recognition sequence. *Dev. Biol. 139*, 227−229.

(14) Williams, E., Williams, G., Gour, B. J., Blaschuk, O. W., and Doherty, P. (2000) A novel family of cyclic peptide antagonists suggests that N-cadherin specificity is determined by amino acids that flank the HAV motif. *J. Biol. Chem. 275*, 4007−4012.

(15) Oberlender, S. A., and Tuan, R. S. (1994) Spatiotemporal profile of N-cadherin expression in the developing limb mesenchyme. *Cell Adhes Commun. 2*, 521−537.

(16) Tavella, S., Raffo, P., Tacchetti, C., Cancedda, R., and Castagnola, P. (1994) N-CAM and N-cadherin expression during in vitro chondrogenesis. *Exp. Cell Res. 215*, 354−362.

(17) DeLise, A. M., and Tuan, R. S. (2002) Alterations in the spatiotemporal expression pattern and function of N-cadherin inhibit cellular condensation and chondrogenesis of limb mesenchymal cells in vitro. *J. Cell. Biochem. 87*, 342−359.

(18) Kim, I. G., Ko, J., Lee, H. R., Do, S. H., and Park, K. (2016) Mesenchymal cells condensation-inducible mesh scaffolds for cartilage tissue engineering. *Biomaterials 85*, 18−29.

(19) Li, R., Xu, J., Wong, D. S. H., Li, J., Zhao, P., and Bian, L. (2017) Self-assembled N-cadherin mimetic peptide hydrogels promote the chondrogenesis of mesenchymal stem cells through inhibition of canonical Wnt/β-catenin signaling. *Biomaterials 145*, 33−43.

(20) Bian, L., Guvendiren, M., Mauck, R. L., and Burdick, J. A. (2013) Hydrogels that mimic developmentally relevant matrix and N-cadherin interactions enhance MSC chondrogenesis. *Proc. Natl. Acad. Sci. U. S. A. 110*, 10117−10122.

(21) Zhu, M., Lin, S., Sun, Y., Feng, Q., Li, G., and Bian, L. (2016) Hydrogels functionalized with N-cadherin mimetic peptide enhance osteogenesis of hMSCs by emulating the osteogenic niche. *Biomaterials 77*, 44−52.

(22) Engler, A. J., Sen, S., Sweeney, H. L., and Discher, D. E. (2006) Matrix elasticity directs stem cell lineage specification. *Cell 126*, 677−689.

(23) Sun, M., Chi, G., Li, P., Lv, S., Xu, J., Xu, Z., Xia, Y., Tan, Y., Xu, J., Li, L., and Li, Y. (2018) Effects of Matrix Stiffness on the Morphology, Adhesion, Proliferation and Osteogenic Differentiation of Mesenchymal Stem Cells. *Int. J. Med. Sci. 15*, 257−268.

(24) Subramanian, A., and Lin, H. Y. (2005) Crosslinked chitosan: its physical properties and the effects of matrix stiffness on chondrocyte cell morphology and proliferation. *J. Biomed. Mater. Res., Part A 75*, 742−753.

(25) Bonab, M. M., Alimoghaddam, K., Talebian, F., Ghaffari, S. H., Ghavamzadeh, A., and Nikbin, B. (2006) Aging of mesenchymal stem cell in vitro. *BMC Cell Biol. 7*, 14.

(26) Hall, B. K., and Miyake, T. (1995) Divide, accumulate, differentiate: cell condensation in skeletal development revisited. *Int. J. Dev Biol. 39*, 881−893.

(27) Chen, W. C., Wei, Y. H., Chu, I. M., and Yao, C. L. (2013) Effect of chondroitin sulphate C on the in vitro and in vivo chondrogenesis of mesenchymal stem cells in crosslinked type II collagen scaffolds. *J. Tissue Eng. Regener. Med. 7*, 665−672.

(28) Goldring, M. B., Tsuchimochi, K., and Ijiri, K. (2006) The control of chondrogenesis. *J. Cell. Biochem. 97*, 33−44.

(29) Salinas, C. N., and Anseth, K. S. (2008) The enhancement of chondrogenic differentiation of human mesenchymal stem cells by enzymatically regulated RGD functionalities. *Biomaterials 29*, 2370−2377.

(30) Re'em, T., Tsur-Gang, O., and Cohen, S. (2010) The effect of immobilized RGD peptide in macroporous alginate scaffolds on TGFbeta1-induced chondrogenesis of human mesenchymal stem cells. *Biomaterials 31*, 6746−6755.

(31) Adams, C. L., Nelson, W. J., and Smith, S. J. (1996) Quantitative analysis of cadherin-catenin-actin reorganization during development of cell-cell adhesion. *J. Cell Biol. 135*, 1899−1911.

(32) Kulyk, W. M., Franklin, J. L., and Hoffman, L. M. (2000) Sox9 expression during chondrogenesis in micromass cultures of embryonic limb mesenchyme. *Exp. Cell Res. 255*, 327−332.

(33) Benya, P. D., Padilla, S. R., and Nimni, M. E. (1978) Independent regulation of collagen types by chondrocytes during the loss of differentiated function in culture. *Cell 15*, 1313−1321.

(34) Buckwalter, J. A., and Mankin, H. J. (1998) Articular cartilage: tissue design and chondrocyte-matrix interactions. *Instr Course Lect 47*, 477−486.

(35) Kiani, C., Chen, L., Wu, Y. J., Yee, A. J., and Yang, B. B. (2002) Structure and function of aggrecan. *Cell Res. 12*, 19−32.

(36) DeLise, A. M., Fischer, L., and Tuan, R. S. (2000) Cellular interactions and signaling in cartilage development. *Osteoarthritis Cartilage 8*, 309−334.

(37) Akiyama, H., Chaboissier, M. C., Martin, J. F., Schedl, A., and de Crombrugghe, B. (2002) The transcription factor Sox9 has essential roles in successive steps of the chondrocyte differentiation pathway and is required for expression of Sox5 and Sox6. *Genes Dev. 16*, 2813−2828.

(38) Smits, P., Li, P., Mandel, J., Zhang, Z., Deng, J. M., Behringer, R. R., de Crombrugghe, B., and Lefebvre, V. (2001) The transcription factors L-Sox5 and Sox6 are essential for cartilage formation. *Dev. Cell 1*, 277−290.

(39) Lefebvre, V., and Dvir-Ginzberg, M. (2017) SOX9 and the many facets of its regulation in the chondrocyte lineage. *Connect. Tissue Res. 58*, 2−14.

DOI: 10.1021/acs.bioconjchem.9b00514
Bioconjugate Chem. 2019, 30, 2417−2426

(40) Topol, L., Chen, W., Song, H., Day, T. F., and Yang, Y. (2009) Sox9 inhibits Wnt signaling by promoting beta-catenin phosphorylation in the nucleus. *J. Biol. Chem. 284*, 3323−3333.

DOI: 10.1021/acs.bioconjchem.9b00514
Bioconjugate Chem. 2019, 30, 2417−2426